Research article

Pralatrexate mediates effective killing of gemcitabine-resistant pancreatic cancer: role of mTOR/4E-BP1 signal pathway

Wanwen Weng [a,b,c,d,e,1], Jiawei Hong [a,b,c,d,1], Kwabena G. Owusu-Ansah [f,g], Bingjie Chen [a,b,c,d], Shusen Zheng [a,b,c,d,**], Donghai Jiang [a,b,c,d,*]

[a] Division of Hepatobiliary and Pancreatic Surgery, Department of Surgery, The First Affiliated Hospital, Zhejiang University School of Medicine, Hangzhou 310003, China
[b] NHC Key Laboratory of Combined Multi-organ Transplantation, Hangzhou 310003, China
[c] Key Laboratory of the Diagnosis and Treatment of Organ Transplantation, Research Unit of Collaborative Diagnosis and Treatment for Hepatobiliary and Pancreatic Cancer, Chinese Academy of Medical Sciences (2019RU019), Hangzhou 310003, China
[d] Key Laboratory of Organ Transplantation, Research Center for Diagnosis and Treatment of Hepatobiliary Diseases, Zhejiang Province, Hangzhou 310003, China
[e] Department of Nuclear Medicine, The First Affiliated Hospital, College of Medicine, Zhejiang University School of Medicine, Hangzhou 310003, China
[f] Department of Internal Medicine, St. Elizabeth Youngstown Hospital, Youngstown, OH, USA
[g] Department of Medicine, Northeastern Ohio Medical University, Rootstown, OH, USA

ARTICLE INFO

ABSTRACT

Gemcitabine is the first-line chemotherapeutic agent for pancreatic cancer. However, gemcitabine-resistance frequently leads to poor prognosis. Exploring new chemotherapeutic agents is important for patients with gemcitabine-resistant pancreatic cancer. In this study, we established a new acquired gemcitabine-resistant pancreatic cancer cell line BxPC-GEM-20 from parental BxPC-3. We found that pralatrexate significantly inhibited the growth of BxPC-GEM-20. The half-maximal inhibitory concentration of pralatrexate on BxPC-GEM-20 cell was about 3.43 ± 0.25 nM. Pralatrexate was found to effectively inhibit the clonal growth of BxPC-GEM-20 cell. Additionally, pralatrexate at 20 mg/kg had an excellent tumor inhibitory effect with an inhibitory rate of 76.92% *in vivo*. This pralatrexate therapy showed good safety profile that with little to no additional influence on the hepatic, renal function as well as body weight changes in nude mice. Pralatrexate was confirmed to prevent cells from entering the G2/M phase, leading to the promotion of apoptosis and autophagy. Further analysis demonstrated that the reduced phosphorylation of mTOR played a significant role in the tumor cell damage caused by pralatrexate. Pralatrexate effectively inhibited the mTOR/4E-BP1 pathway. Activation of mTOR pathway can further obstruct the repressive effect of pralatrexate on gemcitabine-resistant pancreatic cancer. In summary, pralatrexate induces effective inhibition of gemcitabine-resistant pancreatic cancer. This may lead to the expansion of pralatrexate's application and offer benefit to gemcitabine-resistant pancreatic cancer patients in the future.

1. Introduction

Pancreatic cancer (PC), also known as pancreatic ductal adenocarcinoma (PDAC), is currently the seventh leading cause of cancer-related deaths in the western world [1], and is expected to overtake colorectal cancer as the second leading cause of cancer-related death in the United States by 2030 [2]. PC has traits like high degree of malignancy, early metastasis, and late diagnosis, among others [3, 4]. Unfortunately, some

patients have lost the surgery opportunity at the time of diagnosis. Chemotherapy is the preferred option for those kinds of pancreatic cancer treatment [3, 5]. Clinic trials have demonstrated that gemcitabine, a cytidine analogue, is more efficient than 5-fluorouracil (5-FU), a common and basic chemotherapeutic agent for PC [3, 4, 5, 6, 7]. Patients with advanced pancreatic cancer had a median overall survival of 5–6.5 months and a 1-year survival rate of approximately 11–25% when gemcitabine monotherapy had been used [8]. For more than 20 years,

gemcitabine has been used extensively as a frontline chemotherapy agent for PC patients and has been regarded as the gold standard treatment [5] (see Table 1).

However, gemcitabine as monotherapy has been less effective in improving outcomes due to the intrinsic and acquired gemcitabine-resistance [8, 9, 10]. The acquired gemcitabine-resistance in PC often result in poor clinical outcomes [9]. Thus, there have been numerous attempts in gemcitabine combination therapy for advanced PC patients. Currently, combination agents such as gemcitabine/nab-paclitaxel (AG), 5-FU/leucovorin with irinotecan and oxaliplatin regime (FOLFIRINOX) are considered first-line regimen in PC patients [3, 11]. However, besides limited efficiency, these combination agents lead to increased toxicity [11, 12]. Other chemotherapeutic drugs, including cisplatin, epirubicin, fluorouracil and gemcitabine (PEFG), capecitabine with oxaliplatin (CapeOx), gemcitabine, docetaxel, and capecitabine (GTX), etc. might be an alternative option for patients with gemcitabine-resistant pancreatic cancer [9]. Unfortunately, the gemcitabine combination provides a modest improvement of survival, but is associated with more adverse events (AEs) compared with gemcitabine monotherapy [13, 14]. Due to these serious limitations to gemcitabine treatment, two options could be provided in parallel which could potentially offer improvement in the gemcitabine combination regimen or administrating new effective agents.

Antifolate agent which inhibits folate metabolism is one of the anti-tumor drugs. But it is rarely used in the treatment of pancreatic cancer [15]. Although pre-clinical application of pemetrexed (Alimta) has shown synergistic effects in combination with gemcitabine *in vitro*. However, it provides no significant differences in survival rate compared with gemcitabine monotherapy [16]. Pralatrexate is an IV antifolate agent with high affinity for the one carbon-reduced folate carrier and thereby inhibits the enzyme dihydrofolate reductase (DHFR) [17, 18, 19]. Pralatrexate can inhibit the biosynthesis of tetrahydrofolic acid (FH$_4$) and thus theoretically disrupts DNA synthesis contributing to the death of tumor cells [20]. At present, the use of pralatrexate is limited to patients with complex peripheral T-cell lymphoma (PTCL) who have failed other treatments [17, 20]. There is limited data with application of pralatrexate in PC, especially gemcitabine-resistant PC.

Using the Gemcitabine-resistant Pancreatic Cancer (GEM-RPC) cell line BxPC-GEM-20 as a model, we conducted a thorough screening of compounds with possible antitumor action. This allowed us to conclude that pralatrexate had a favorable inhibitory effect on tumor growth. Our investigation proved that pralatrexate had an excellent antitumor effect on gemcitabine-resistant PC cell lines. Pralatrexate can effectively prevent cancer cells from entering the G2/M phase, enhance apoptosis in a manner dependent on dose, and provide acceptable safety profile *in vivo*. Exploring these features can provide a novel treatment perspective for patients with gemcitabine-resistant pancreatic cancer.

2. Materials and methods

2.1. Cell culture maintenance and mice

HPNE, CFPAC-1, AsPC-1, BxPC-3 and PANC-1 cell line were obtained from National Collection of Authenticated Cell Cultures (Shanghai, China). BxPC-3 and AsPC-1 cells were maintained in RPMI 1640 medium with additional 10% fetal bovine serum (FBS), CFPAC-1 was maintained in IMDM medium (BasalMedia, Shanghai, China) supplemented with 10% FBS. PANC-1 and HPNE cells were cultured in DMEM medium with additional 10% FBS. All cells were cultured in a 37 °C humidified incubator.

Male athymic nude (BALB/C Nude) mice aged 5 weeks were obtained from the Zhejiang University Animal Facility. Animal experiments and care were in accordance with the Guidelines of the Zhejiang University Animal Care Committee. The Ethics Committee of the First Affiliated Hospital of Zhejiang University's School of Medicine also gave its approval to all animal tests. All mice were fed in specific pathogen-free vivarium.

2.2. Establishment of acquired GEM-RPC cell line

A new acquired GEM-RPC cell line BxPC-GEM-20 was established from BxPC-3. The BxPC-3 cells were initially exposed to a stepwise rise of gemcitabine concentrations from 0.5 nM to 20 nM. The acquired gemcitabine-resistant cell line BxPC-GEM-20, which proliferated properly in a 20 nM gemcitabine concentration, was maintained in RPMI 1640 with additional 20 nM gemcitabine and 10% FBS.

2.3. Drug screening and cell treatments

The kinase inhibitor library (L1200, Selleck, USA) included nearly 2000 small-molecule compounds was used to screen which one had a desirable inhibitory effect on BxPC-GEM-20 cells. Cells were seeded in 96 well plates and exposed to various compounds at 50nM. After 72 h incubation, the morphology and growth feature of BxPC-GEM-20 cells were examined by inverted microscope. The compound that could completely kill BxPC-GEM-20 cells at 50nM was further studied.

Pralatrexate (50mg, #MB4343-2, Meilunbio, China) and Gemcitabine HCL (1g, #MB1113, Meilunbio, China) were dissolved in DMSO and water, respectively. MHY1485 (10 mM/1 mL in DMSO, #HY-B0795, MCE, China).

The cells were uniformly seeded in the corresponding medium for 24 h in 37 °C humidified incubator. Then they were given different doses of agents according to the research design.

2.4. CCK8 assay and colony-forming assay of pralatrexate's effect

Various cells were uniformly divided and seeded in the 96 well culture plates. Different drug treatments strategies were applied to the

Table 1. English abbreviation.

Abbreviation	Full Name
4E-BP1	eIF4E-binding protein 1
5-FU	5-fluorouracil
AEs	adverse events
AG	gemcitabine/nab-paclitaxel chemotherapy
ALT	alanine aminotransferase
AST	aspartate aminotransferase
BSA	bovine serum albumin
CapeOx	capecitabine with oxaliplatin chemotherapy
CD31/PECAM-1	platelet/endothelial cell adhesion molecule-1
Cr	creatinine
CV	Crystal Violet
DHFR	enzyme dihydrofolate reductase
FBS	fetal bovine serum
FH$_4$	tetrahydrofolic acid
FITC	fluorescein isothiocyanate
FOLFIRINOX	5-FU/leucovorin with irinotecan and oxaliplatin chemotherapy
GEM-RPC	Gemcitabine-resistant pancreatic cancer
GTX	gemcitabine, docetaxel, and capecitabine chemotherapy
IC$_{50}$	half maximal inhibitory concentration
IR	inhibition rate
mTOR	mechanistic target of rapamycin
MTX	methotrexate
PARP	poly ADP-ribose polymerase
PBS	phosphate-buffered saline
PC	pancreatic cancer
PDAC	Pancreatic ductal adenocarcinoma
PEFG	cisplatin, epirubicin, fluorouracil and gemcitabine chemotherapy
PI	propidium iodide
PTCL	peripheral T-cell lymphoma
RT	room temperature

specified columns after 24 h incubation. And after 72 h culture, 100 μL of CCK-8 reagent (CCK8: medium = 1:9) was added to each well and then cultured for another 1 h. The absorbance of each well was then measured at 450nm using a microplate reader (Bio-Rad, USA).

Various cells were maintained for 10–14 days with different drug regimens in 6-cm culture dish with a total of $8*10^3$–$1*10^4$ cells. The plates were washed twice with phosphate buffer solution (PBS), and the separated cells were then fixed for 10 min in methanol and then stained for another 10 min with Crystal Violet (CV). Then pictures of tumor cell colonies were photographed after plates were washed with water.

2.5. Assay of cell cycle in pralatrexate's effect

After 72 h of exposure to the drug in 37 °C humidified incubator, cells were gathered and washed two times with PBS, then fixed with 70% ethanol diluted in PBS. Before being analyzed, cells underwent a 0.5-hour incubation period in PBS containing 40 μg/L of propidium iodide (PI) and 100 μg/mL of RNase-A at room temperature. A Coulter Epics V equipment (Beckman Coulter, USA) was used to determine DNA content and cell cycle distribution. And to analyze the distribution of the cell cycle, the Modifit LT 5.0 software (Verity Software House, USA) was applied.

2.6. Assay of apoptosis in pralatrexate's effect

Cell apoptosis was detected using Annexin V/PI apoptosis detection Kit (Vazyme, China) according to the manufacturer's instructions. The cells were collected and washed twice after 36–48 h of treatment. Thereafter they were suspended in 400 μL of binding buffer, 10 μL of PI solution and 5 μL of Annexin V antibody conjugated with fluorescein isothiocyanate (FITC). After 15 min at 4 °C in a dark environment of incubation in the mixture, apoptosis rate was measured by flow cytometry. Apoptosis was quantified using FlowJo-V10 software (BD Biosciences, San Jose, CA, USA).

2.7. Western blot analysis and antibodies source

The antibodies used in west blot were listed as follows: CDK6 (#db807, Diagbio, China); PARP (#9542), Cyclin D1 (#55506), Cyclin B1 (#12231), Cleaved-PARP (#5625), CDK2 (#18048), mTOR (#2983), p-mTOR (#5536), p-4E-BP1 (#2855), 4E-BP1 (#9644), Caspase-3 (#9668), phospho-Histone H3 (pHH3) (#53348), Histone H2A (γH2A.x) (#12349), Cleaved Caspase-3 (#9664), GAPDH (#5174) were purchased from Cell Signaling Technology (USA); SQSTM1/p62 (#A19700) and LC3I/LC3II (#A5618) were obtained from ABclonal Technology (Wuhan, China); goat anti-mouse and goat anti-rabbit IgG peroxidase conjugated secondary antibodies (#31460 and #31430, Thermo-Pierce, USA). The protein samples were added to 4–20% SurePAGE gels (15 wells) (GenScript, China) and transferred to PVDF membranes after protein separation. Incubate the membrane with the primary antibodies mentioned above. After washing with TBST (0.1% (v/v) Tween 20 in TBS), the membranes were incubated with secondary antibodies and then stained with enhanced chemiluminescence.
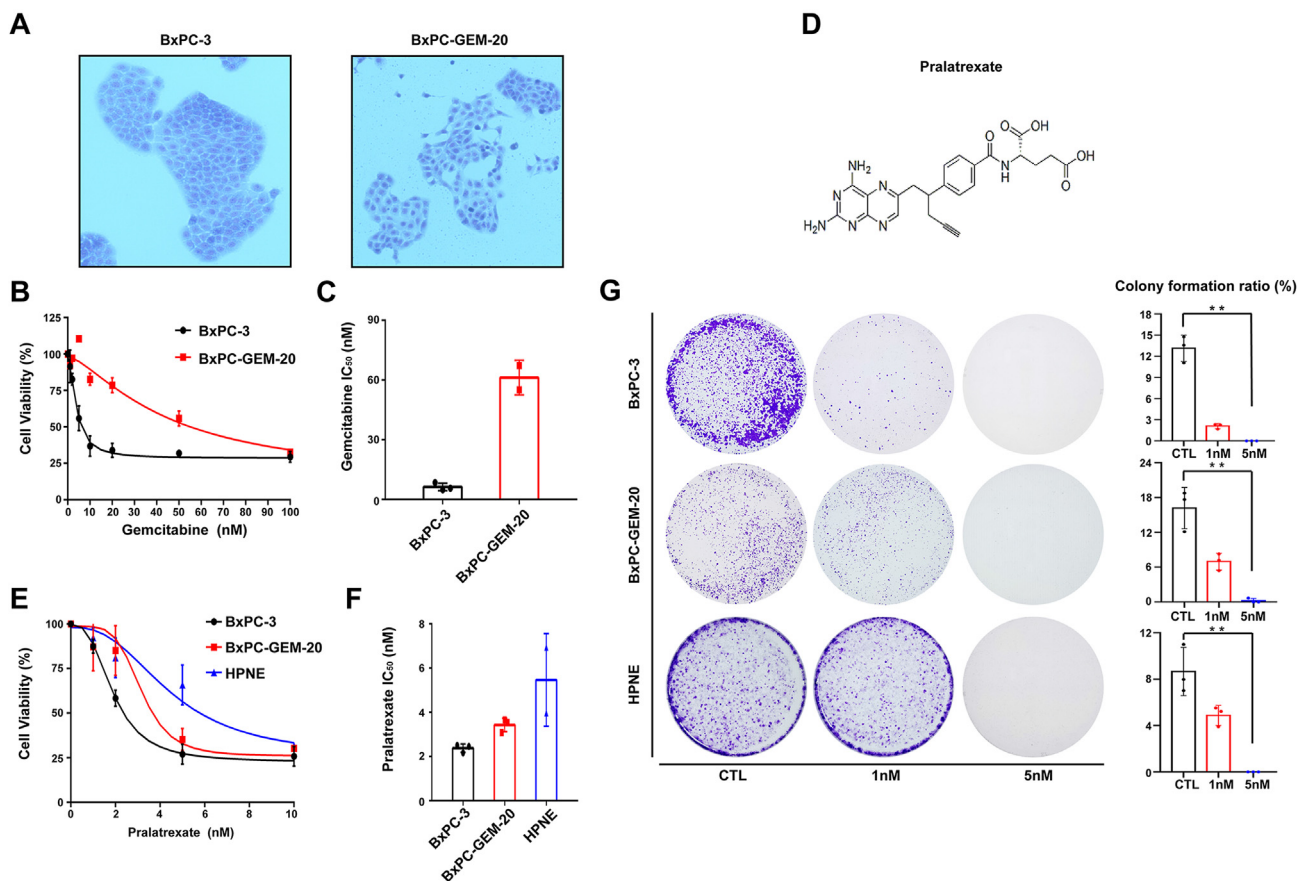
Figure 1. Pralatrexate inhibits the growth of gemcitabine-resistant pancreatic cancer cells *in vitro* (A) Morphological images of BxPC-3 and BxPC-GEM-20 cell lines (×100) (B–C) BxPC-3 and BxPC-GEM-20 were exposed to a series of concentrations of gemcitabine for 72 h, the IC_{50} of gemcitabine was determined after 72 h treatment; Data are represented as the mean ± SD (n = 3 per group) (D) The structural formula of pralatrexate (E–F) BxPC-3, BxPC-GEM-20 and HPNE were exposed to pralatrexate for 72 h, the IC_{50} of pralatrexate was determined after 72 h treatment, Data are represented as the mean ± SD (n = 3 per group) (G) Colony formation of BxPC-3, BxPC-GEM-20 and HPNE with various pralatrexate dose treatments. Relative quantification is shown. Data are represented as the mean ± SD (n = 3 per group). CTL, control.
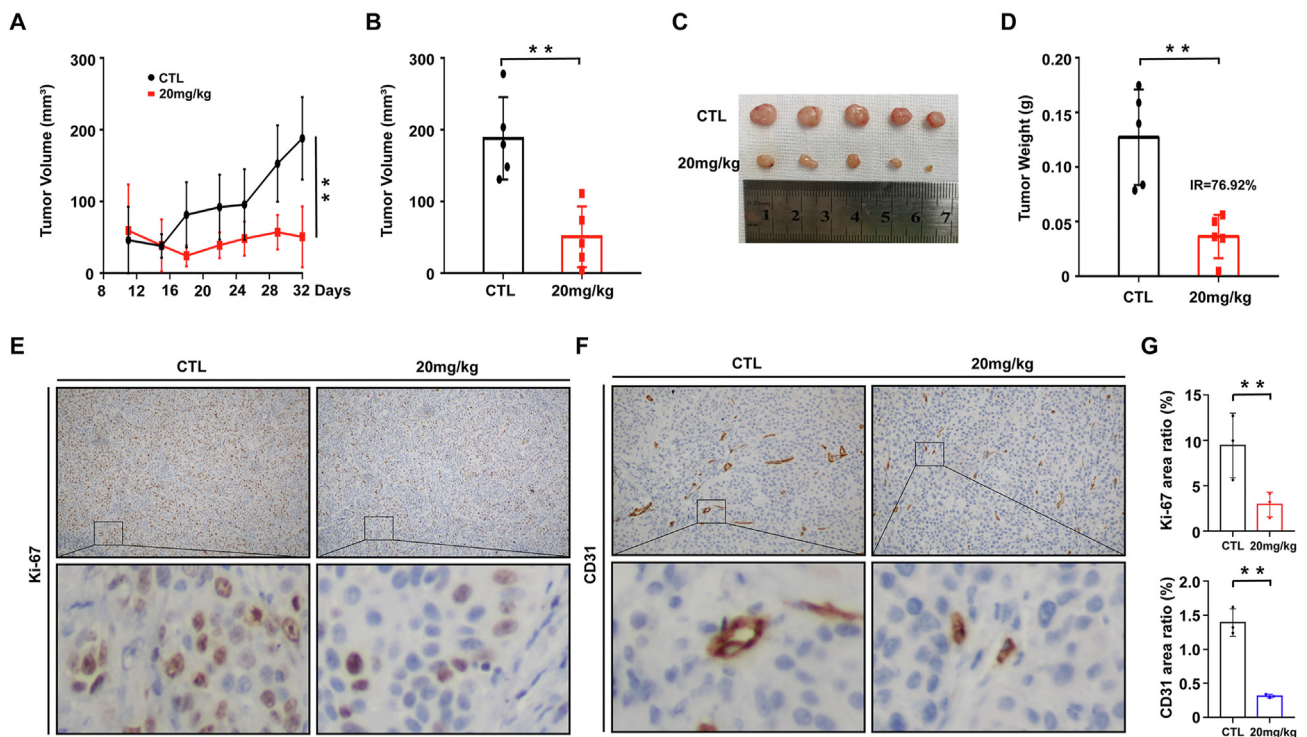
Figure 2. Pralatrexate inhibits BxPC-GEM-20 xenograft growth. Nude mice bearing BxPC-GEM-20 tumors were treated with or without pralatrexate (A) The process of tumor volume change in the two groups. Data are represented as the mean ± SD (n = 5 per group) (B) Tumor volume of the two groups at the end of experiments. Data are represented as the mean ± SD (n = 5 per group) (C) Tumor mass of the two groups with different treatments (D) Tumor weight of the two groups after mice sacrificed. The IR in pralatrexate was calculated compared with the control group. Data are represented as the mean ± SD (n = 5 per group) (E–F) The Ki-67 and CD31 immunohistochemical staining (the graph up: ×100; the graph below, ×400) of the tumor (G)The area ratio of Ki67 and CD31. Relative quantification is shown. Data are represented as the mean ± SD (n = 3 per group) *P < 0.05; **P < 0.01; CTL, control; IR, inhibition rate.

2.8. Immunofluorescent staining

The GEM-RPC cells from vehicle and pralatrexate monotherapy treatment groups in 6-well plates were washed three times. The cells were then fixed with 4% paraformaldehyde (PFA) for 20 min, followed by 20 min of incubation with 0.5% TritonX-100 in PBS. Subsequently, the cells were incubated with blocking buffer (4% bovine serum albumin (BSA) (Absin, Shanghai, China) in PBS) for 1h at room temperature. All cells were washed with PBS three times after permeabilization and blocking. Primary antibodies were diluted at the suggested ratios and incubated at 4 °C overnight. Then, all cells were washed with PBST at room temperature three times. Appropriate secondary antibodies (#AS007) (ABclonal, Wuhan, China) were added and incubated for 1 h at room temperature in dark environment. Finally, the cells were treated with DAPI (MCE, China) for 5 min in a dark environment and washed with PBST at room temperature. The confocal microscope (OLYMPUS IX83-FV3000-OSR, Tokyo, Japan) were used to photograph pictures.

2.9. Immunohistochemistry

First, the tumor specimen after vehicle or pralatrexate treatment were fixed in formalin and then placed in paraffin. Paraffin-embedded samples were cut into slices, separated and rehydrated. The activity of endogenous peroxidase was deactivated with 3% H_2O_2 in methanol. The antigen was retrieved at 100 °C using citrate buffer (Beyotime, Shanghai, China), then cooled and exposed to the designated primary antibody (Ki67, # ab16667, Abcam, UK; CD31, # ab182981, Abcam, UK) at 4 °C overnight. On the next day, the samples were washed with PBS three times and incubated for 1 h at 37 °C with a secondary antibody conjugated with a horseradish peroxidase (HRP) (OriGene Technologies, Rockville, MD, USA) for 1 h, and then DAB (Zsbio, Beijing, China) was used for microscopic observation.

2.10. Evaluation of the pralatrexate's therapeutic efficacy in vivo

BxPC-GEM-20 cells were harvested and implanted into the homozygous nude athymic mice left side of flanks (100μL containing 8×10^6 cells in saline). 11 days after implantation, the mice were randomly divided into two groups, each of which had 5 mice, and were given different treatments: (i) vehicle; (ii) Pralatrexate at 20 mg/kg, i. v. Pralatrexate was dissolved in saline. Pralatrexate and vehicle group were injected with pralatrexate or saline twice a week for totally 3 weeks. After the mice were sacrificed, the length(L) and width(W) of the tumor and the weight of the mice were measured, and the mice tumor volume(V) was calculated by the following formula ($\pi \approx 3.14$):

$$V = (\pi * L * W^2)/6$$

The tumor tissues were removed and weighed after the animals were sacrificed. Liver, kidney and blood samples were also harvested. A Hitachi 7600 automated analyzer (Hitachi, Japan) was used to measure serum alanine aminotransferase (ALT), aspartate transferase (AST), creatinine (Cr) and blood glucose levels. And the formula for calcutating inhibition rate (IR) was as follow:

IR= (mean tumor weight of the vehicle group - mean tumor weight of the pralatrexate group)/mean tumor weight of the vehicle group *100%

2.11. Statistical analysis

All quantitative results were presented as means ± standard errors. P < 0.05 (*), P < 0.01 (**), P < 0.001 (***) or P < 0.0001 (****) was considered as the statistical significance. The data of the two groups were compared using the student t test, and the multi-treatment group was compared using the one-way analysis of variance (ANOVA). SPSS 22.0 (IBM, USA) was used for statistical analysis of the data.
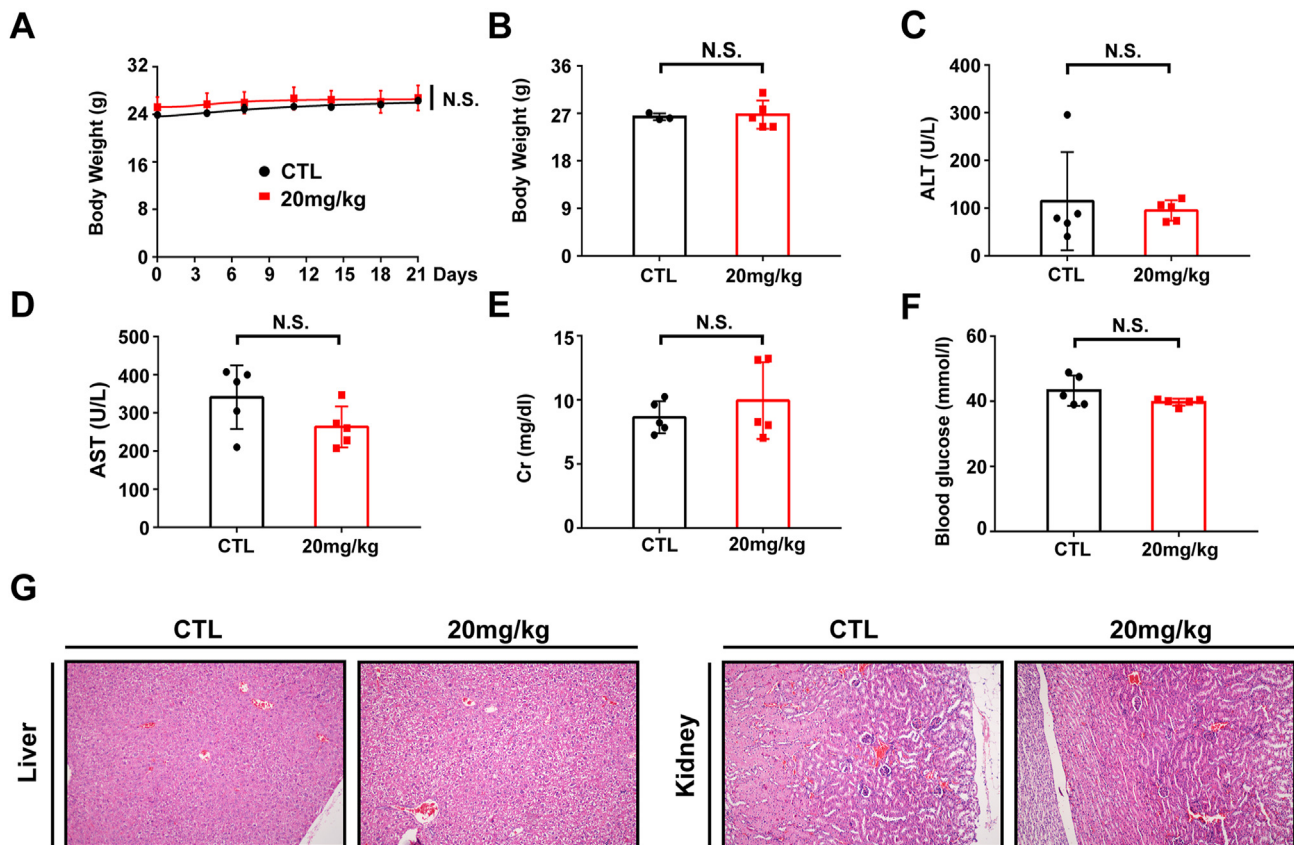
Figure 3. Pralatrexate brings few additional adverse effects *in vivo* (A) Body weight of mice during the treatment process. Data are represented as the mean ± SD (n = 5 per group) (B) Body weight of mice after mice sacrificed. Data are represented as the mean ± SD (n = 5 per group) (C–F) Serum ALT, AST, Cr and blood glucose measured in two groups after mice sacrificed. Data are represented as the mean ± SD (n = 5 per group) (G) The liver and kidney tissue with HE staining (×100). N.S. $P > 0.05$; CTL, control.

3. Results

3.1. Pralatrexate effectively inhibits the growth of GEM-RPC cells in vitro

In this research, we established a novel GEM-RPC cell line BxPC-GEM-20 from parental BxPC-3 cells. The STR sequencing confirmed BxPC-3 as the parent cell line of BxPC-GEM-20 (Supplementary Material 1). BxPC-GEM-20 cells had looser intercellular connections compared with BxPC-3 (Figure 1A). The half-maximal inhibitory concentration (IC_{50}) of gemcitabine on BxPC-3 and BxPC-GEM-20 were 6.38 ± 1.09 nM, 61.14 ± 6.15 nM, respectively (Figure 1B–C, $P = 0.0014$). BxPC-GEM-20 showed more tolerance to gemcitabine.

The structural formula of pralatrexate was seen in Figure 1D. Pralatrexate-induced cytotoxicity was determined in BxPC-3, BxPC-GEM-20 and the human pancreatic ductal cell HPNE, with measured IC_{50} at 2.38 ± 0.15, 3.43 ± 0.25 and 5.46 ± 1.48 nM, respectively (Figure 1E-F, $P = 0.0447$). Concurrently, colony-forming assay was used to investigate the inhibitory effect of pralatrexate on all three pancreatic cells. As demonstrated in Figure 1. G, the colony-forming assay showed significant dose-dependent reduction in the number and size of cells in the pralatrexate monotherapy groups. These results confirmed the efficacy of the inhibitory effect of pralatrexate monotherapy on gemcitabine-resistant pancreatic cancer cells' growth at a nanomolar level.

Pralatrexate inhibits BxPC-GEM-20 xenograft tumor *in vivo*.

Previous experiments have revealed the effectiveness of pralatrexate in killing pancreatic cancer cell lines *in vitro*. Hence, the clinical concern regarding the replication of this phenomenon *in vivo*. Animal experiments were subsequently performed. As depicted in Figure 2A-D, pralatrexate effectively inhibits BxPC-GEM-20 xenograft tumors' growth, with a final tumor volume of 188.1 ± 25.76mm [3] in the vehicle and 50.65 ±

19.02mm [3] in the pralatrexate groups (Figure 2B, $P = 0.0026$). As shown in Figure 2D, the final tumor weight was 0.13 ± 0.04 g in the vehicle group and 0.03 ± 0.02 g in the pralatrexate groups ($P = 0.0029$). Compared to the vehicle group, 20 mg/kg pralatrexate therapy markedly suppressed tumor growth with an IR of 76.92%. Furthermore, the expressions of Ki-67 in resected GEM-20 xenograft tumors were analyzed (Figure 2E). The proportion of Ki-67 positive cells was notably reduced, suggesting less proliferation in tumors in the pralatrexate group. Platelet/endothelial cell adhesion molecule-1 (PECAM-1, CD31), a marker of angiopoiesis and junction between adjacent cells [21, 22], was also remarkably reduced in the pralatrexate group. This illustrated the decreased angiogenesis caused by pralatrexate (Figure 2F). These results suggest that pralatrexate has a strong inhibitory effect on tumor growth and vascularization *in vivo*.

Pralatrexate at therapeutic dose causes acceptable adverse effects *in vivo*.

Next, we evaluated the toxicity of pralatrexate *in vivo*. The body weights as well as serum ALT, AST, Cr and blood glucose concentrations of the mice were used to evaluate toxicity. We found that pralatrexate at therapeutic dose did not exert any significant nephrotoxic or hepatotoxic effects in mice. The results are shown in Figure 3A-B. The use of pralatrexate at 20 mg/kg did not significantly inhibit body weight in mice. In addition, the serum ALT level of the two groups were 114.38 ± 92.13 U/L, 94.82 ± 19.38 U/L ($P = 0.5476$). AST levels were 340.70 ± 74.69 U/L, 263.00 ± 47.83 U/L, respectively ($P = 0.1178$). Creatinine levels were 8.63 ± 1.12 mg/dL, 9.94 ± 2.68 mg/dL ($P = 0.3937$) and blood glucose concentrations were 43.26 ± 4.18 mmol/L, 39.74 ± 0.95 mmol/L, respectively ($P = 0.4206$) (Figure 3C–F). Moreover, serological detections showed that the adverse effects on the liver and kidney function after the injection of pralatrexate were within acceptable range. Hepatic
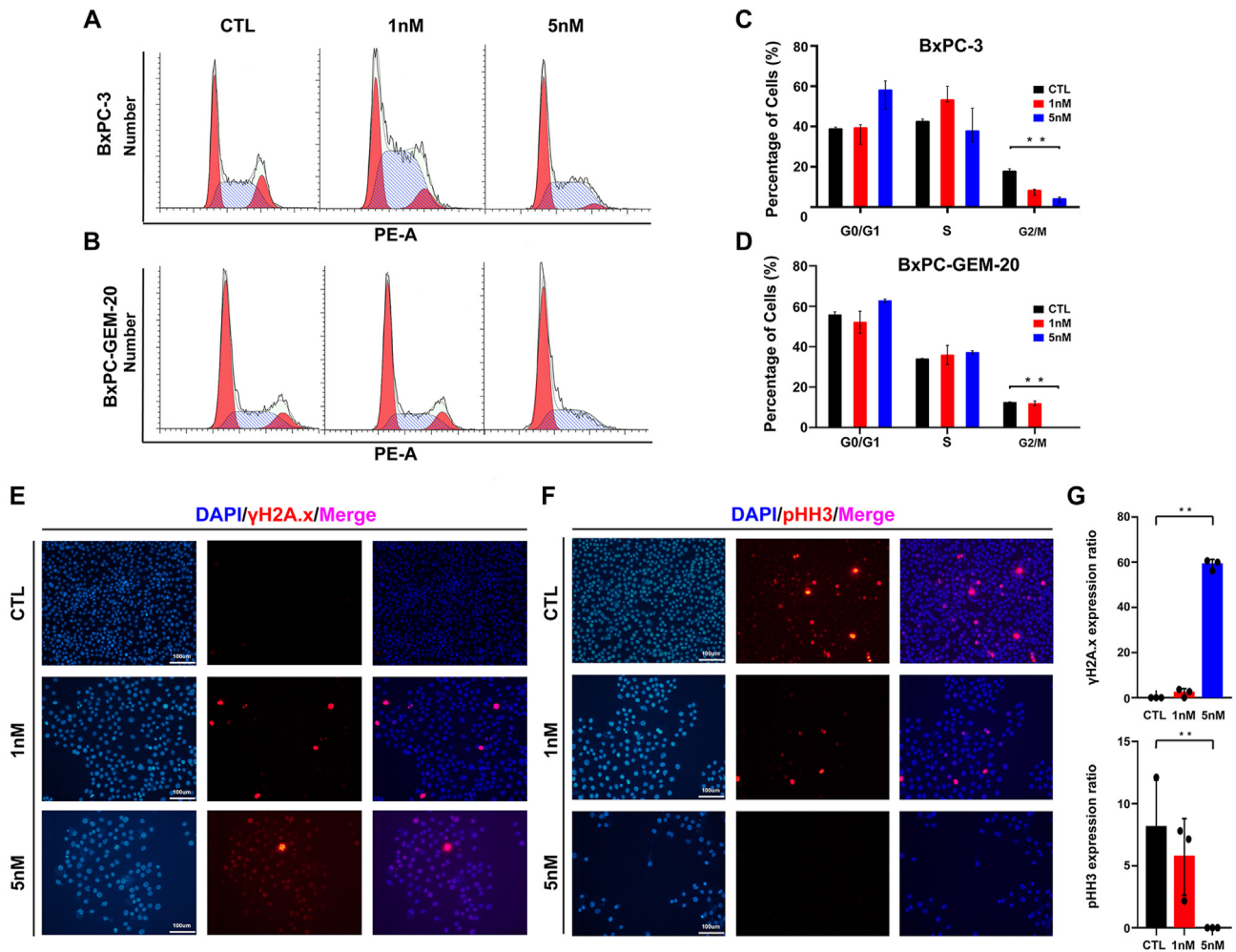
Figure 4. Pralatrexate prevents cancer cells from entering G2/M phase (A–D) Cell cycle analysis of BxPC-3 and BxPC-GEM-20 cells and different cell cycle phase histogram. Data are represented as the mean ± SD (n = 3 per group) (E–F) the γH2A.x and pHH3 immunofluorescence assay (×200) in BxPC-GEM-20 cell after different treatments for 48 h (G) The expression ratio of γH2A.x and pHH3. Data are represented as the mean ± SD (n = 3 per group). **P < 0.01; CTL, control.

and renal HE staining also showed that pralatrexate had no significant effect on liver and kidney morphology (Figure 3G). Our results confirmed that pralatrexate inhibits tumor growth in BxPC-GEM-20 xenografts without severe adverse effects.

Pralatrexate prevents cancer cells from entering G2/M phase.

As depicted in Figure 4A-D, 5 nM pralatrexate remarkably prevented a significant number of cells from entering G2/M phase in a dose-dependent pattern, from 19.04% to 4.11% (BxPC-3) and 10.01%–0% (BxPC-GEM-20). Interestingly, the rate of BxPC-GEM-20 G2/M phase in the 5nM pralatrexate group was 0% consistently in our three independent repeat assays. Histone H2AX (γH2A.x), was used as a marker for DNA damage [23]. Over-expression of γH2A.x in pralatrexate treated group suggested its ability to cause significant damage to DNA (Figure 4E). In addition, histone H3 phosphorylation (pHH3) [24] was detected to evaluate the effect on cell cycle arrest. The decrease of pHH3 expression in the therapy group proved that pralatrexate could lead to abnormal mitosis in a dose-dependent manner (Figure 4F). The decrease in CDK2, CDK6, Cyclin D1, and Cyclin B1 levels also suggest the obstruction of cell entering G2/M phase [25, 26]. Consequently, increased pralatrexate concentration led to significantly down-regulated expression of these cycle proteins (Figure 5E). This result confirmed the role of pralatrexate preventing cells from entering G2/M phase in gemcitabine-resistant PC.

3.2. Pralatrexate promotes apoptosis and autophagy

As shown in Figure 5A-D, results from the flow cytometric analysis indicated that 5nM pralatrexate significantly increased the ratio of apoptotic BxPC-3 and BxPC-GEM-20 cells compared to the vehicle group (39.57%–5.84%, BxPC-3, p < 0.0001) and (44.16%–6.72%, BxPC-GEM-20, p = 0.0043). Subsequently, the expression level of several regulatory proteins related to apoptosis of BxPC-GEM-20 cells was analyzed (Figure 5F). The increased level of poly ADP-ribose polymerase (C-PARP/ PARP-1) and cleavage of caspase-3 (C-Caspase-3/active Caspase-3) corresponded with cell apoptosis [27, 28]. The levels of cleavage PARP-1 and active Caspase-3 were significantly increased in the pralatrexate monotherapy group. In summary, pralatrexate administration mediates tumor cell apoptosis. Further analysis showed that pralatrexate promotes the activation of LC3-I to LC3-II and downregulates p62 in BxPC-GEM-20 cells, further confirming that pralatrexate promotes autophagy (Figure 5G).

Suppression of mTOR plays a crucial role in the antitumor effect of pralatrexate.

We further explored whether pralatrexate affects the mTOR signaling pathway as mTOR plays a vital role in autophagy [29]. Our results show that pralatrexate can effectively reduce the total amount and inhibit the phosphorylation of mTOR (Figure 6A). As a downstream molecule of mTOR, the expression and phosphorylation of eIF4E-binding protein 1
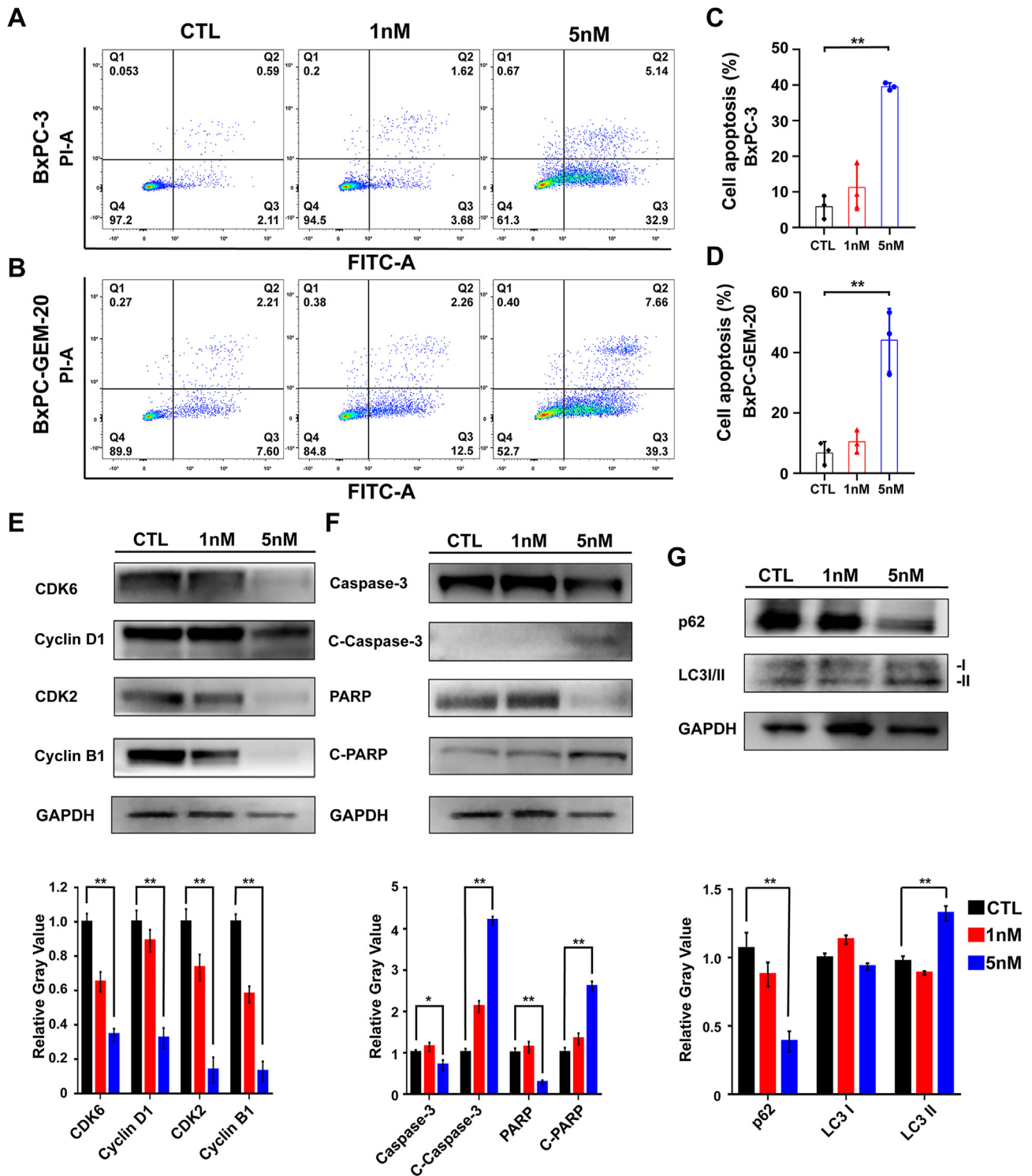
Figure 5. Pralatrexate induces tumor cell apoptosis and autophagy (A–D) Apoptosis assay of BxPC-3 and BxPC-GEM-20 cell and the cell apoptosis rate histogram. Data are represented as the mean ± SD (n = 3 per group) (E) Western blot analysis of Cyclin B1, Cyclin D1, CDK2 and CDK6 in BxPC-GEM-20 cell after different treatments for 72 h. Relative quantification is shown. Data are represented as the mean ± SD (n = 3 per group), Uncropped west blot images in supplement 2 (F) Western blot analysis of PARP, cleaved-PARP, caspase3 and cleaved-caspase3 in BxPC-GEM-20 cell after different treatments for 72 h. Relative quantification is shown. Data are represented as the mean ± SD (n = 3 per group), Uncropped west blot images in supplement 2 (G) Western blot analysis of p62 and LC3 I/II in BxPC-GEM-20 cell after different treatments for 72 h. Relative quantification is shown. Data are represented as the mean ± SD (n = 3 per group), Uncropped west blot images in supplement 2. *P < 0.05; **P < 0.01; CTL, control.

(4E-BP1) was also reduced (Figure 6A). MHY1485 (MHY), a mTOR acti-vator [30], had no obvious inhibitory effect on BxPC-GEM-20 cell growth at 5 μM but had a strong effect in promoting mTOR and 4E-BP1 synthesis

and phosphorylation (Figure 6B–C). To determine whether the mTOR signaling pathway contributes to the anti-tumor effect of pralatrexate, we used MHY in combination with pralatrexate for BxPC-GEM-20 cell. In the
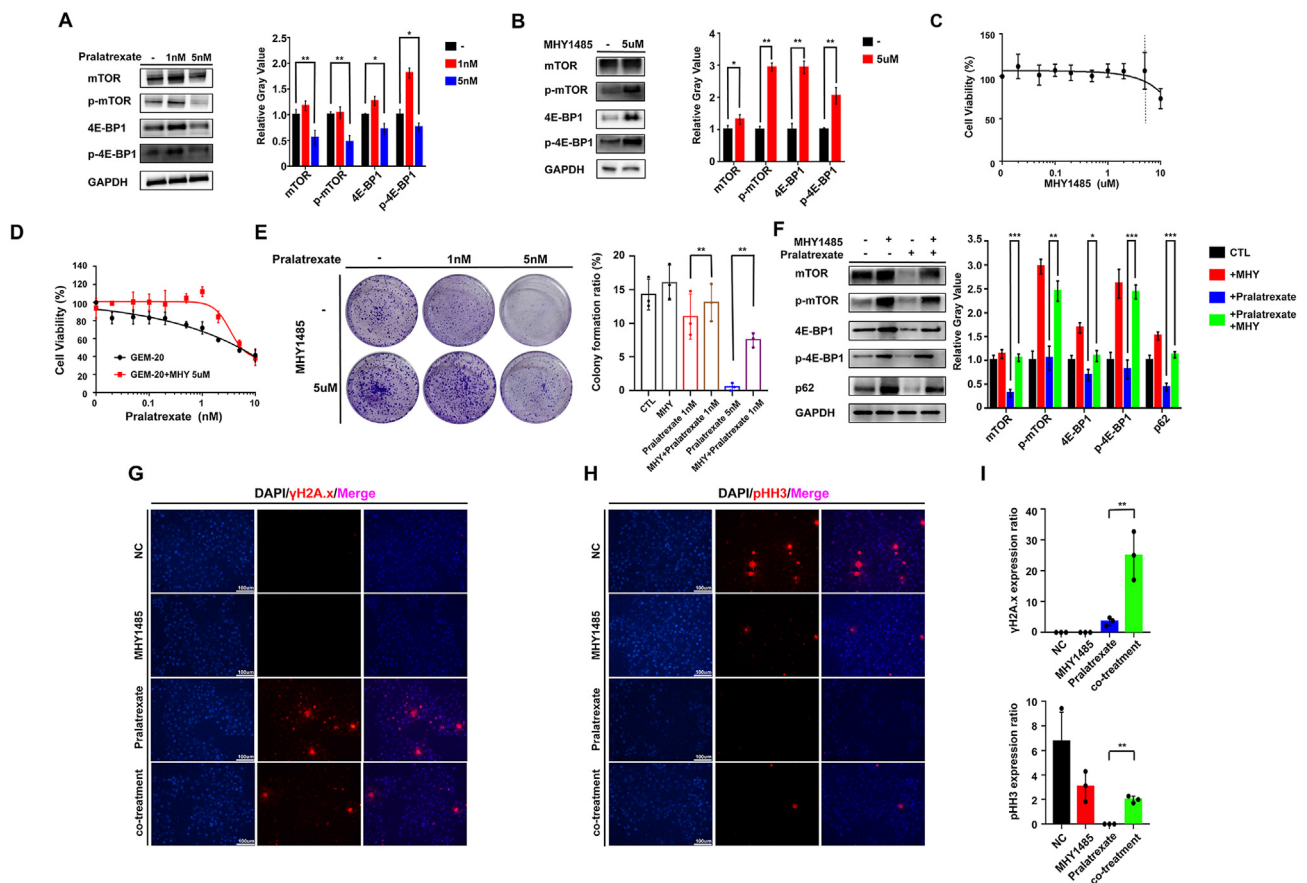
Figure 6. Inhibition of mTOR plays a significant role in the antitumor effect of pralatrexate (A–B) Western blot analysis of mTOR pathway-related proteins, mTOR, phosphorylation mTOR, 4E-BP1 and phosphorylation 4E-BP1 in BxPC-GEM-20 cell after different treatments for 72 h. Relative quantification is shown. Data are represented as the mean ± SD (n = 3 per group), Uncropped west blot images in supplement 2 (C) BxPC-GEM-20 was exposed to MHY for 72 h, the cytotoxicity of MHY was determined after 72 h treatment (D) BxPC-GEM-20 was exposed to pralatrexate with or without 5 μM MHY1485 for 72 h, the cell viabilities were determined (E) Colony formation of BxPC-GEM-20 with different treatments. Data are represented as the mean ± SD (n = 3 per group) (F) Western blot analysis of mTOR pathway-related proteins, mTOR, phosphorylation mTOR, 4E-BP1 and phosphorylation 4E-BP1, and autophagy-related proteins, p62, in BxPC-GEM-20 cell after different treatments for 72 h, Uncropped west blot images in supplement 2 (G–H) the γH2A.x and pHH3 immunofluorescence assay (×200) in BxPC-GEM-20 cell after different treatments for 48 h (I) The expression ratio of γH2A.x and pHH3. Relative quantification is shown. Data are represented as the mean ± SD (n = 3 per group). *P < 0.05; **P < 0.01; ***P < 0.001; CTL, control.

presence of MHY, the tolerance of BxPC-GEM-20 cells to pralatrexate were greatly enhanced (Figure 6D-E). Further assay confirmed that the mTOR inhibition of pralatrexate could be obstructed by MHY (Figure 6F). The alteration of p-mTOR/mTOR ratio means change of kinase activity. The alteration ratios of p-mTOR/total mTOR were 0.05 ± 0.01, 1.33 ± 0.27 in pralatrexate monotherapy and co-treatment groups, respectively (P = 0.0025). In the presence of MHY, pralatrexate-induced overexpression of γH2A.x was reduced (Figure 6G). However, the expression of pHH3 was recovered in the co-treatment group (Figure 6H). These results demonstrated that the inhibition of mTOR signal pathway played a critical role in the antitumor effect of pralatrexate.

Pralatrexate's influence on primary gemcitabine-resistant pancreatic cancer.

CFPAC-1 showed a desirable tolerance to gemcitabine compared with BxPC-3, AsPC-1, PANC-1 and BxPC-GEM-20 cells (Figure 7A). CFPAC-1 cells were hence considered as intrinsic gemcitabine-resistant pancreatic cancer cells to explore pralatrexate's antitumor effect. Interestingly, we found that pralatrexate also had a robust inhibitory effect on CFPAC-1 (Figure 7B). Pralatrexate also inhibited the mTOR pathway in CFPAC-1 (Figure 7C). And no obvious inhibitory effect on CFPAC-1 cell growth was observed with 2 μM of MHY (Figure 7D). Subsequently, we proved that CFPAC-1 cell greatly enhances its tolerance to pralatrexate in the presence of 2 μM MHY (Figure 7E). This further established that pralatrexate-induced cytotoxicity could also be obstructed by MHY. Our

results proved that pralatrexate had a strong inhibitory effect on GEM-RPC cell lines. In a nutshell, mTOR/4E-BP1 signal pathway can be inhibited by pralatrexate, promoting its anti-tumor effect (Figure 7F).

4. Discussion

Our investigation confirmed that pralatrexate provides an acceptable safety profile at therapeutic dose in experimental nude mice. Pralatrexate could prevent gemcitabine-resistant PC cells from entering G2/M phase and promote the apoptosis of tumor cells effectively. Subsequent studies have shown that the inhibition of mTOR runs a significant role in the anti-tumor effect of pralatrexate in PC cells. Our study is the first to prove that pralatrexate can be used as a potential chemotherapy agent in gemcitabine-resistant PC.

As described previously, the emerging gemcitabine resistance is one of the major challenges in the current treatment of pancreatic cancer. It is therefore necessary to explore new chemotherapeutic agents for the treatment of gemcitabine-resistant PC. Our study demonstrates that pralatrexate has a favorable inhibitory effect on acquired/primary gemcitabine-resistant pancreatic cancer cell lines. The therapeutic effectiveness and security *in vivo* are the most momentous point in clinical research. The various AEs associated with pralatrexate include stomatitis, mucositis, bone marrow suppression (neutropenia, anemia and thrombocytopenia), nausea, constipation, edema, cough, epistaxis,
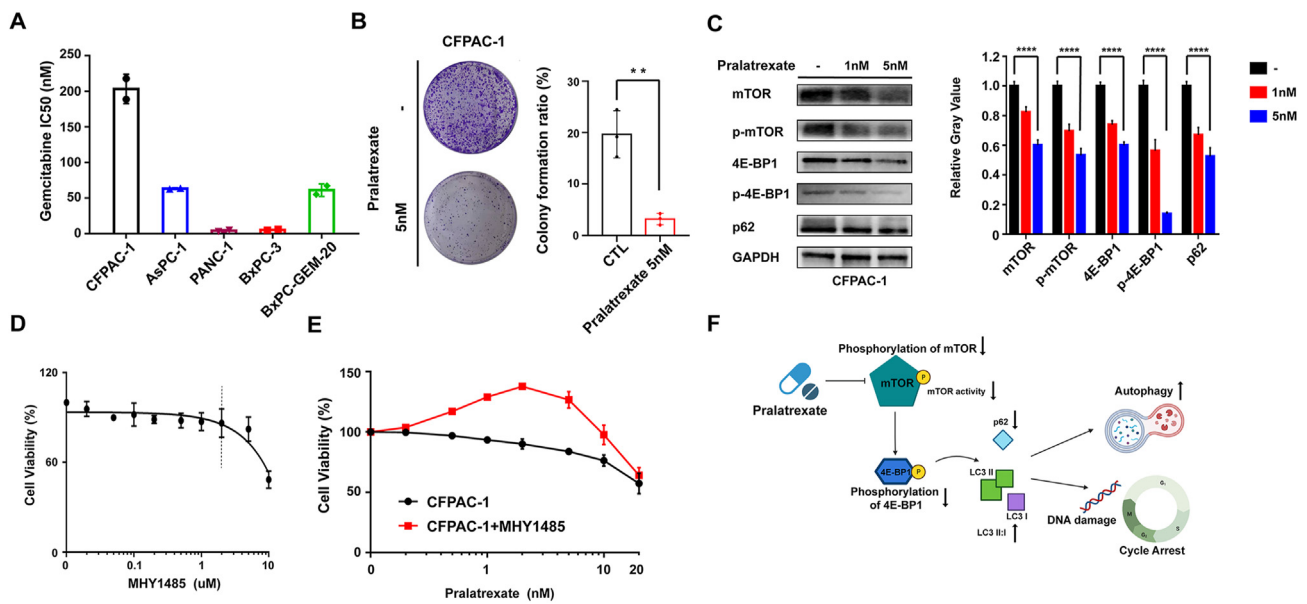
Figure 7. Pralatrexate represses intrinsic gemcitabine-resistant pancreatic cancer and its' antitumor mechanisms (A) the IC_{50} of gemcitabine in CFPAC-1, AsPC-1, PANC-1 BxPC-3 and BxPC-GEM-20 were determined after gemcitabine treatment for 72 h. Data are represented as the mean $\pm$ SD (n = 3 per group) (B) Colony formation of CFPAC-1 with different treatments. Data are represented as the mean $\pm$ SD (n = 3 per group) (C) Western blot analysis of mTOR pathway-related proteins, mTOR, phosphorylation mTOR, 4E-BP1, phosphorylation 4E-BP1 and SQSTM1/p62 in CFPAC-1 cell after different treatments for 72 h. Relative quantification is shown. Data are represented as the mean $\pm$ SD (n = 3 per group), Uncropped west blot images in supplement 2 (D) CFPAC-1 was exposed to MHY for 72 h, the cytotoxicity of MHY was determined after 72 h treatment. Data are represented as the mean $\pm$ SD (n = 3 per group) (E) CFPAC-1 was exposed to pralatrexate with or without 2 μM MHY1485 for 72 h, the cell viabilities were determined. Data are represented as the mean $\pm$ SD (n = 3 per group) (F) Pralatrexate's antitumor mechanisms by inhibiting mTOR function and phosphorylation. $**P < 0.01$; $****P < 0.0001$; CTL, control.

vomiting, diarrhea, etc [17, 31, 32]. We found acceptable biochemical results with pralatrexate as monotherapy in xenograft tumor models compared with the vehicle group. The body weight as well as serum liver and kidney function indexes of the nude mice were within normal range. These outcomes validate pralatrexate monotherapy as appropriate and safe for gemcitabine-resistant pancreatic cancer patients. Consequently, pralatrexate might be an effective agent for treatment of GEM-RPC cells *in vivo* with minimal toxicity. *Pralatrexate monotherapyPralatrexate monotherapy* regimen may also lay a foundation for expanding the clinical application of pralatrexate in gemcitabine-resistant pancreatic cancer patient in the future. This study offers a novel perspective into the clinical application of pralatrexate in anticancer treatment.

The mTOR pathway is one of the significant signaling pathways in tumorigenesis in the majority of human cancers [29, 33]. And mTOR participates in the phosphorylation of 4E-BP1 at multiple sites thus mediating autophagy [34]. It has been reported that the mTOR pathway can mediate drug resistance by enhancing autophagy [35]. and plays a significant role in the tumorigenesis of pancreatic carcinoma [36]. It is abnormally activated in pancreatic cancer and is related to tumor glycolysis (Warburg effect) and other glucose metabolism process [37]. In addition, the mTOR signaling pathway also promotes gemcitabine resistance in PC. Shingo Kagawa and colleagues confirmed the involvement of the mTOR pathway in gemcitabine resistance induced by Annexin II in pancreatic cancer cells [38]. Our study demonstrates the feasibility of pralatrexate as a chemotherapeutic agent to inhibit the phosphorylation of mTOR in GEM-RPC cells, and activating mTOR can antagonize the antitumor effect of pralatrexate. Moreover, pralatrexate could induce autophagy by promoting the expression of LC3 and reducing the expression of p62. It has been suggested that promoting autophagy contributes to the pralatrexate induced effective killing of GEM-RPC cells. As an antifolate agent, pralatrexate can inhibit the biosynthesis of FH_4 by inhibiting DHFR and thus disrupts DNA synthesis. Elena Silva and colleagues found that the deficiency and inhibition of folic acid can lead to the inhibition of mTOR in the fetus [39].

Likewise, our outcomes also demonstrated that pralatrexate can inhibit the mTOR/4E-BP1 pathway. There is a potential influence relationship between folic acid synthesis and the mTOR signaling pathway. However, the specific mechanism of the two pathways in cancer cells is still unclear and deserves further investigation. From our perspective, further studies are needed to reveal the effect of pralatrexate on mTOR phosphorylation, related signaling pathway and folic acid metabolism in the future.

In short, this study suggests that pralatrexate is an effective treatment strategy for gemcitabine-resistant pancreatic cancer which might expand the clinic application of pralatrexate and offer benefits to gemcitabine-resistant pancreatic cancer patients.

Declarations

Author contribution statement

Wanwen Weng; Jiawei Hong: Performed the experiments; Analyzed and interpreted the data; Wrote the paper.

Kwabena G. Owusu-Ansah: Analyzed and interpreted the data; Wrote the paper.

Bingjie Chen: Contributed reagents, materials, analysis tools or data.

Donghai Jiang; Shusen Zheng: Conceived and designed the experiments.

Funding statement

Data availability statement

Data included in article/supp. material/referenced in article.

Declaration of interest's statement

The authors declare no conflict of interest.

Additional information

Supplementary content related to this article has been published online at https://doi.org/10.1016/j.heliyon.2022.e12064.

References

[1] H. Sung, J. Ferlay, R.L. Siegel, et al., Global cancer statistics 2020: GLOBOCAN estimates of incidence and mortality worldwide for 36 cancers in 185 countries, CA A Cancer J. Clin. 71 (3) (2021) 209–249.

[2] L. Rahib, B.D. Smith, R. Aizenberg, A.B. Rosenzweig, J.M. Fleshman, L.M. Matrisian, Projecting cancer incidence and deaths to 2030: the unexpected burden of thyroid, liver, and pancreas cancers in the United States, Cancer Res. 74 (11) (2014) 2913–2921.

[3] S. Zeng, M. Pöttler, B. Lan, R. Grützmann, C. Pilarsky, H. Yang, Chemoresistance in pancreatic cancer, Int. J. Mol. Sci. 20 (18) (2019).

[4] H.A. Burris 3rd, M.J. Moore, J. Andersen, et al., Improvements in survival and clinical benefit with gemcitabine as first-line therapy for patients with advanced pancreas cancer: a randomized trial, J. Clin. Oncol. 15 (6) (1997) 2403–2413.

[5] U. Klaiber, C.S. Leonhardt, O. Strobel, C. Tjaden, T. Hackert, J.P. Neoptolemos, Neoadjuvant and adjuvant chemotherapy in pancreatic cancer, Langenbeck's Arch. Surg. 403 (8) (2018) 917–932.

[6] F. Di Costanzo, P. Carlini, L. Doni, et al., Gemcitabine with or without continuous infusion 5-FU in advanced pancreatic cancer: a randomised phase II trial of the Italian oncology group for clinical research (GOIRC), Br. J. Cancer 93 (2) (2005) 185–189.

[7] W. Park, A. Chawla, E.M. O'Reilly, Pancreatic cancer: a review, JAMA 326 (9) (2021) 851–862.

[8] G. von Wichert, T. Seufferlein, G. Adler, Palliative treatment of pancreatic cancer, Am. J. Dig. Dis. 9 (1) (2008) 1–7.

[9] D. Sarvepalli, M.U. Rashid, A.U. Rahman, et al., Gemcitabine: a review of chemoresistance in pancreatic cancer, Crit. Rev. Oncog. 24 (2) (2019) 199–212.

[10] W. Li, Y. Zhu, K. Zhang, et al., PROM2 promotes gemcitabine chemoresistance via activating the Akt signaling pathway in pancreatic cancer, Exp. Mol. Med. 52 (3) (2020) 409–422.

[11] T. Conroy, F. Desseigne, M. Ychou, et al., FOLFIRINOX versus gemcitabine for metastatic pancreatic cancer, N. Engl. J. Med. 364 (19) (2011) 1817–1825.

[12] V. Kunzmann, J.T. Siveke, H. Algül, et al., Nab-paclitaxel plus gemcitabine versus nab-paclitaxel plus gemcitabine followed by FOLFIRINOX induction chemotherapy in locally advanced pancreatic cancer (NEOLAP-AIO-PAK-0113): a multicentre, randomised, phase 2 trial, Lancet Gastroenterol. Hepatol. 6 (2) (2021) 128–138.

[13] J.P. Neoptolemos, D.H. Palmer, P. Ghaneh, et al., Comparison of adjuvant gemcitabine and capecitabine with gemcitabine monotherapy in patients with resected pancreatic cancer (ESPAC-4): a multicentre, open-label, randomised, phase 3 trial, Lancet (London, England) 389 (10073) (2017) 1011–1024.

[14] C. Sun, D. Ansari, R. Andersson, D.Q. Wu, Does gemcitabine-based combination therapy improve the prognosis of unresectable pancreatic cancer? World J. Gastroenterol. 18 (35) (2012) 4944–4958.

[15] D. Levêque, R. Santucci, B. Gourieux, R. Herbrecht, Pharmacokinetic drug-drug interactions with methotrexate in oncology, Expet Rev. Clin. Pharmacol. 4 (6) (2011) 743–750.

[16] J.F. Seitz, L. Dahan, P. Ries, Pemetrexed in pancreatic cancer, Oncology 18 (13 Suppl 8) (2004) 43–47.

[17] O.A. O'Connor, B. Pro, L. Pinter-Brown, et al., Pralatrexate in patients with relapsed or refractory peripheral T-cell lymphoma: results from the pivotal PROPEL study, J. Clin. Oncol. 29 (9) (2011) 1182–1189.

[18] E.S. Wang, O. O'Connor, Y. She, A.D. Zelenetz, F.M. Sirotnak, M.A. Moore, Activity of a novel anti-folate (PDX, 10-propargyl 10-deazaaminopterin) against human lymphoma is superior to methotrexate and correlates with tumor RFC-1 gene expression, Leuk. Lymphoma 44 (6) (2003) 1027–1035.

[19] E. Marchi, L. Paoluzzi, L. Scotto, et al., Pralatrexate is synergistic with the proteasome inhibitor bortezomib in in vitro and in vivo models of T-cell lymphoid malignancies, Clin. Cancer Res.: An Off. J. Am. Assoc. Cancer Res. 16 (14) (2010) 3648–3658.

[20] Pralatrexate for lymphoma, Aust. Prescr. 42 (2) (2019) 77.

[21] P. Lertkiatmongkol, D. Liao, H. Mei, Y. Hu, P.J. Newman, Endothelial functions of platelet/endothelial cell adhesion molecule-1 (CD31), Curr. Opin. Hematol. 23 (3) (2016) 253–259.

[22] A. Woodfin, M.B. Voisin, S. Nourshargh, PECAM-1: a multi-functional molecule in inflammation and vascular biology, Arterioscler. Thromb. Vasc. Biol. 27 (12) (2007) 2514–2523.

[23] J. Fillingham, M.C. Keogh, N.J. Krogan, GammaH2AX and its role in DNA double-strand break repair, Biochem. Cell Biol. 84 (4) (2006) 568–577.

[24] İ. Elmaci, M.A. Altinoz, R. Sari, F.H. Bolukbasi, Phosphorylated histone H3 (PHH3) as a novel cell proliferation marker and prognosticator for meningeal tumors: a short review, Appl. Immunohistochem. Mol. Morphol. AIMM : AIMM 26 (9) (2018) 627–631.

[25] G.I. Shapiro, Cyclin-dependent kinase pathways as targets for cancer treatment, J. Clin. Oncol. 24 (11) (2006) 1770–1783.

[26] R.L. Sutherland, C.K. Watts, E.A. Musgrove, Cyclin gene expression and growth control in normal and neoplastic human breast epithelium, J. Steroid Biochem. Mol. Biol. 47 (1-6) (1993) 99–106.

[27] M. Rose, J.T. Burgess, K. O'Byrne, D.J. Richard, E. Bolderson, PARP inhibitors: clinical relevance, mechanisms of action and tumor resistance, Front. Cell Dev. Biol. 8 (2020), 564601.

[28] A.G. Porter, R.U. Jänicke, Emerging roles of caspase-3 in apoptosis, Cell Death Differ. 6 (2) (1999) 99–104.

[29] R.A. Saxton, D.M. Sabatini, mTOR signaling in growth, metabolism, and disease, Cell 168 (6) (2017) 960–976.

[30] Y.J. Choi, Y.J. Park, J.Y. Park, et al., Inhibitory effect of mTOR activator MHY1485 on autophagy: suppression of lysosomal fusion, PLoS One 7 (8) (2012), e43418.

[31] C.Z. Jennifer, J. Sara Mohamed, A. Salma, F. Francine, Pralatrexate injection for the treatment of patients with relapsed or refractory peripheral T-cell lymphoma, Expet Rev. Hematol. 13 (6) (2020) 577–583.

[32] O.A. O'Connor, S. Horwitz, P. Hamlin, et al., Phase II-I-II study of two different doses and schedules of pralatrexate, a high-affinity substrate for the reduced folate carrier, in patients with relapsed or refractory lymphoma reveals marked activity in T-cell malignancies, J. Clin. Oncol. 27 (26) (2009) 4357–4364.

[33] D. Mossmann, S. Park, M.N. Hall, mTOR signalling and cellular metabolism are mutual determinants in cancer, Nat. Rev. Cancer 18 (12) (2018) 744–757.

[34] H. Xiang, J. Zhang, C. Lin, L. Zhang, B. Liu, L. Ouyang, Targeting autophagy-related protein kinases for potential therapeutic purpose, Acta Pharm. Sin. B 10 (4) (2020) 569–581.

[35] R.M. Usman, F. Razzaq, A. Akbar, et al., Role and mechanism of autophagy-regulating factors in tumorigenesis and drug resistance, Asia Pac. J. Clin. Oncol. 17 (3) (2021) 193–208.

[36] S. Ebrahimi, M. Hosseini, S. Shahidsales, et al., Targeting the akt/PI3K signaling pathway as a potential therapeutic strategy for the treatment of pancreatic cancer, Curr. Med. Chem. 24 (13) (2017) 1321–1331.

[37] Y. Guo, H. Zhu, M. Weng, H. Zhang, C. Wang, L. Sun, CC-223, NSC781406, and BGT226 exerts a cytotoxic effect against pancreatic cancer cells via mTOR signaling, Front. Pharmacol. 11 (2020), 580407.

[38] S. Kagawa, S. Takano, H. Yoshitomi, et al., Akt/mTOR signaling pathway is crucial for gemcitabine resistance induced by Annexin II in pancreatic cancer cells, J. Surg. Res. 178 (2) (2012) 758–767.

[39] E. Silva, F.J. Rosario, T.L. Powell, T. Jansson, Mechanistic target of rapamycin is a novel molecular mechanism linking folate availability and cell function, J. Nutr. 147 (7) (2017) 1237–1242.